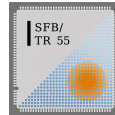


# RQCD Lattice Simulations

G. Bali, V. Braun, P. Bruns, S. Collins, A. Cox, M. Diehl, M. Engelhardt, B. Gläßle, M. Göckler, M. Gruber, F. Hutzler, P. Korcyl, B. Lang, B. Musch, E. Scholz, J. Simeth, P. Wein, T. Wurm, J.-H. Zhang, C. Zimmermann, ...

- RQCD, CLS and SFB/TRR-55
- Standard objects: masses and decay constants, e.g.,  $D_{s0}^*(2317)$  and  $D_{s1}(2460)$ ; GPDs; ...
- Coordinate space methods and DAs (Ji 2013, Braun & Mueller 2008)
- TMDs and DPDs
- QCD in strong magnetic fields
- Conclusion

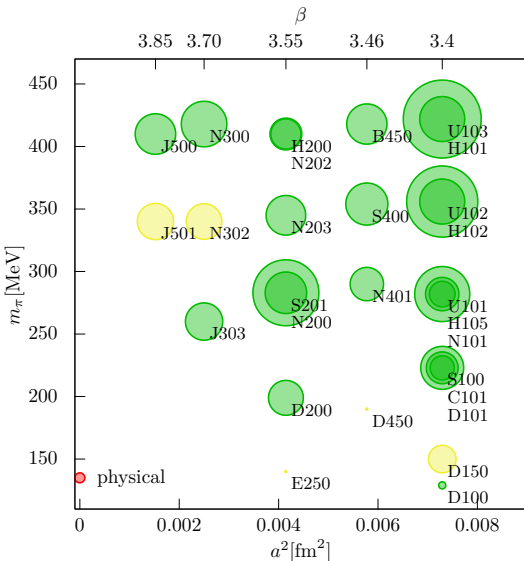


**RQCD:** The Regensburg (& associates) lattice group

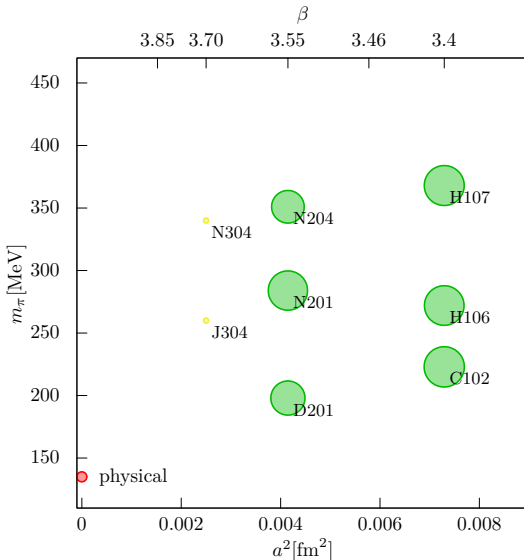
**CLS:** The main systematic uncertainties are meanwhile due to discretization errors. Rapidly increasing topological autocorrelation times for decreasing  $a \Rightarrow$  Lüscher and Schaefer suggested simulations with open boundary conditions  $\Rightarrow$  CLS is an international collaboration pooling its computer resources. Regensburg and Wuppertal are members.

**SFB/TRR-55:** An interdisciplinary research center of Regensburg and Wuppertal University focused on LQCD, Applied Mathematics and HPC plus many external lattice collaborations (e.g. TMDC)

# Ensembles with $m_u + m_d + m_s = \text{physical}$



## Ensembles with $m_s = \text{physical}$



half of QPACE 3 (developed together with Intel and Fujitsu)



## Standard observables I: Moments of GPDs

$$h(P_1) + \Gamma^*(q_1) \rightarrow h(P_2) + \Gamma(q_2)$$

with  $\Delta_\mu = q_{2\mu} - q_{1\mu}$ ,  $t = \Delta^2$ ,  $P_\mu = (P_{1\mu} + P_{2\mu})/2$   
and  $\xi = -Q^2/2P \cdot q$

**Spin  $\frac{1}{2}$  - the nucleon** (modulo gauge links)

$$\begin{aligned} & \int \frac{dz^-}{2\pi} e^{ix\bar{P}^+ z^-} \langle P_2 | \bar{q}(-\frac{1}{2}z) \gamma^+ q(\frac{1}{2}z) | P_1 \rangle \Big|_{z^+=0, z_\perp=0} \\ &= \frac{1}{P^+} \left[ H_q(x, \xi, t) \bar{N}(P_2) \gamma^+ N(P_1) + E_q(x, \xi, t) \bar{N}(P_2) \frac{i\sigma^{+\alpha} \Delta_\alpha}{2M} N(P_1) \right] \end{aligned}$$

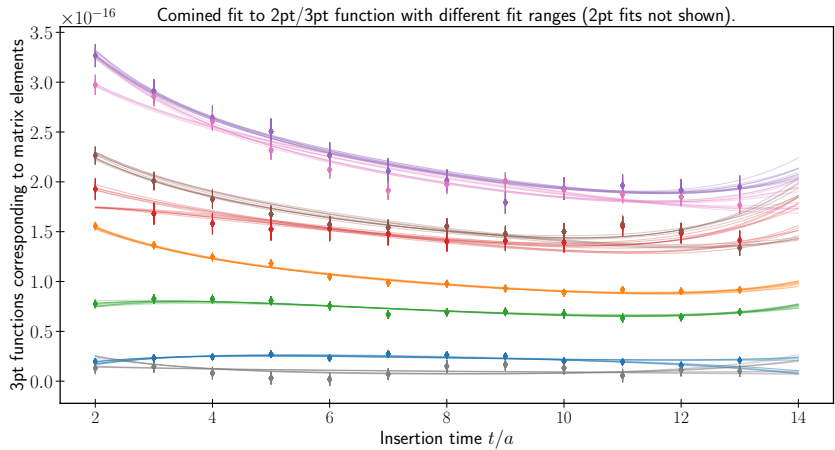
$$\begin{aligned}
\langle p' \lambda | \mathcal{O}^{\{\mu_1 \mu_2\}} | p \lambda \rangle &= P^{\{\mu_1 \langle \langle \gamma^{\mu_2} \rangle \rangle} A_{20}(t) \\
&+ \frac{i}{2m} P^{\{\mu_1 \langle \langle \sigma^{\mu_2}\}^\alpha \rangle \rangle} \Delta_\alpha B_{20}(t) - (2\xi)^2 C_{20}(t) \\
H^{(2)}(\xi, t) &= \int_{-1}^1 dx x H(x\xi, t) = A_{20}(t) + (2\xi)^2 C_{20}(t) \\
E^{(2)}(\xi, t) &= \int_{-1}^1 dx x E(x\xi, t) = B_{20}(t) - (2\xi)^2 C_{20}(t) \\
\mathcal{O}^{\{\mu_1 \mu_2\}} &= \bar{q}(0) \Gamma^{\{\mu_1} i \overset{\leftrightarrow}{D}^{\mu_2\}} q(0) \\
\Gamma^{\mu_1} &= \gamma^{\mu_1}, \gamma^{\mu_1} \gamma_5 \\
F(b_T) &= \frac{1}{(2\pi)^2} \int d^2 \Delta_T e^{-ib_T \cdot \Delta_T} F(\Delta_T)
\end{aligned}$$

M. Diehl and P. Hägler, hep-ph/0504175  
 parton density, expressed in terms of GPDs

$$\begin{aligned}
 & \frac{1}{(2\pi)^2} \int d^2 \Delta_\perp e^{ib_\perp \cdot \Delta_\perp} \int \frac{dz^-}{2\pi} e^{ix\bar{P}^+ z^-} \langle P_2 | \bar{q}(-\frac{1}{2}z) \gamma^+ [1 + \vec{s} \cdot \vec{\gamma}] \gamma_5 q(\frac{1}{2}z) | P_1 \rangle \Big|_{z^+=0}^{z_\perp=0} \\
 &= \frac{1}{2} \left[ F + s^i F_T^i \right] \\
 &= \frac{1}{2} \left[ H - S^i \epsilon^{ij} b^j \frac{1}{m} E' - s^i \epsilon^{ij} b^j \frac{1}{m} (E'_T + 2\tilde{H}'_T) \right. \\
 &\quad \left. + s^i S^i \left( H_T - \frac{1}{4m^2} \Delta_b \tilde{H}_T \right) + s^i (2b^i b^j - b^2 \delta^{ij}) S^j \frac{1}{m^2} \tilde{H}''_T \right]
 \end{aligned}$$

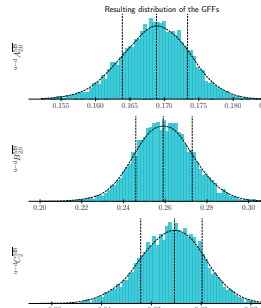
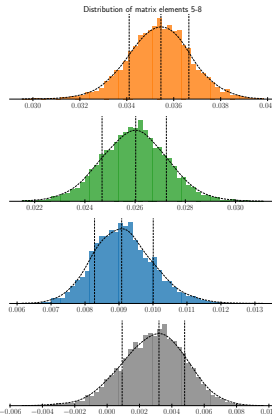
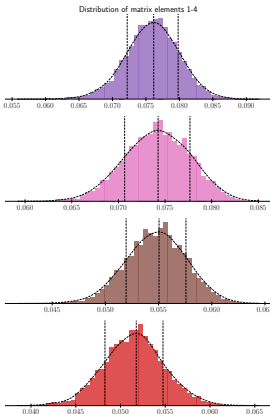
has a simple interpretation:

- $S^i \epsilon^{ij} b^j$  coupling of proton spin to quark angular momentum
- $s^i \epsilon^{ij} b^j$  coupling of quark spin to quark angular momentum
- $s^i S^i$  coupling of quark spin and proton spin

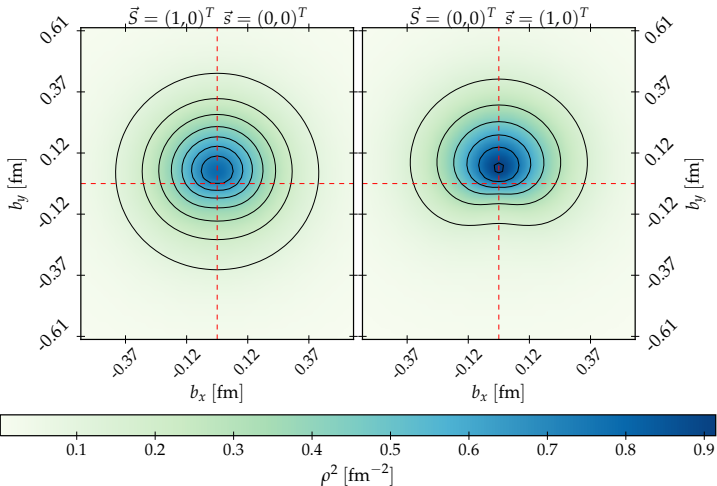


results for the different correlators

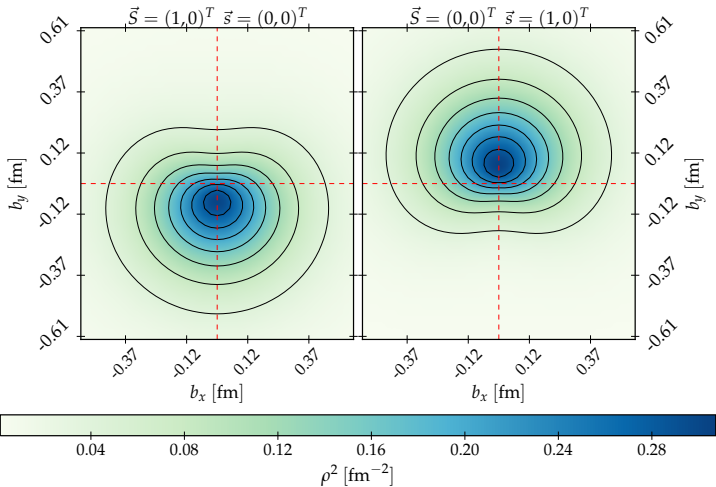
R. Rödl et al.



distribution of extrapolated results many fits, defining the systematic error R. Rödl et al.



transverse densities for u quarks



transverse densities for d quarks

Standard observables II:

$D_{s0}^*(2317)$  and  $D_{s1}(2460)$  masses and decay constants

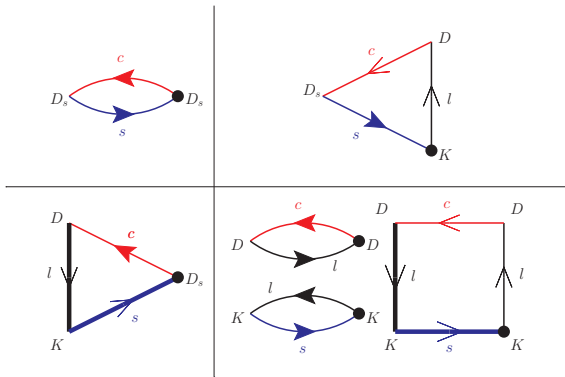
$N_f = 2$ ; physical masses; large statistics; QPACE 1;

S. Collins and A. Cox et al. 1706.01247

These resonances couple strongly to  $D + K$ . Therefore one has to work with mixed states, meaning with a matrix of correlators.

Aim:

- (i) FLAG corrected QCD masses:  $m_{D_s^*}^{QCD} = m_{D_s^*} - \delta m_{D_s^*}^{QED}$
- (ii) decay constants

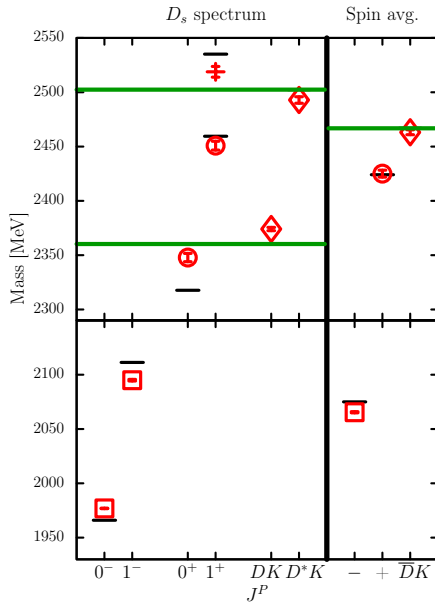


charm, strange, light: red, blue, black lines

stochastic propagators: lines with filled arrows

sequential stochastic propagators: two lines with open arrows

stochastic source: black dot



	$f_S^{0+}$	$f_V^{0+}$	$f_A^{1+}$
This work LQCD hep-lat/0604001	241(4)(2)(+12)(10) 340(110)	114(2)(0)(+5)(10) 200(50)	194(3)(4)(+5)(10)
<i>B</i> -decays+HQS hep-ph/0410301		74(11)	166(20)
<i>B</i> -decays+HQS hep-ph/0305038		67(13)	
<i>B</i> -decays+HQS hep-ph/0605073		58-86	130-200
QM hep-ph/0107047		440	410
QM hep-ph/0312232		122-154	
LF QM hep-ph/0310359		71	117
LF QCDSR hep-ph/0505195*	225(25)		225(25)
<i>DK</i> -molecule 0705.0892		67.1(4.5)	144.5(11.1)
LF QM 1103.2973		74.4 <sup>+10.4</sup> <sub>-10.6</sub>	159 <sup>-36</sup> <sub>+32</sub>
QM 1203.4362		119	165
QCDSR 1506.01993	333(20)		245(17)

\* Colangelo et al. "... favours  $D_{sJ}^*(2317)$  and  $D_{sJ}(2460)$  as ordinary mesons"

Other approaches to calculate hadron structure:

1.) Large Momentum Effective Theory (LaMET) X. Ji et al.

$$\tilde{q}(x, \Lambda, p^z) = \int \frac{dz}{4\pi} e^{ixp^z z} \langle p | \bar{\psi}(0, 0_\perp, z) \gamma^z L(z, 0) \psi(0) | p \rangle$$

gauge link  $L(z, 0)$     hadron momentum  $p^\mu = (p^0, 0, 0, p^z)$   
UV cutoff  $\Lambda$

Results are plagued by artefacts for  $p^z \leq 1 \text{ GeV}$ .

Ideas for improved formulations are needed. Two suggestions:

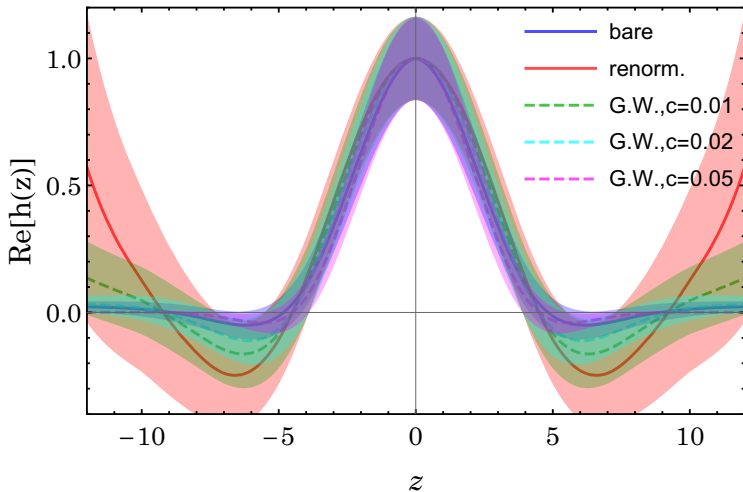
- (i) modified definitions
- (ii) momentum smearing

A Gaussian weight suppresses long distance artefacts but does not require recalculation of the matching functions

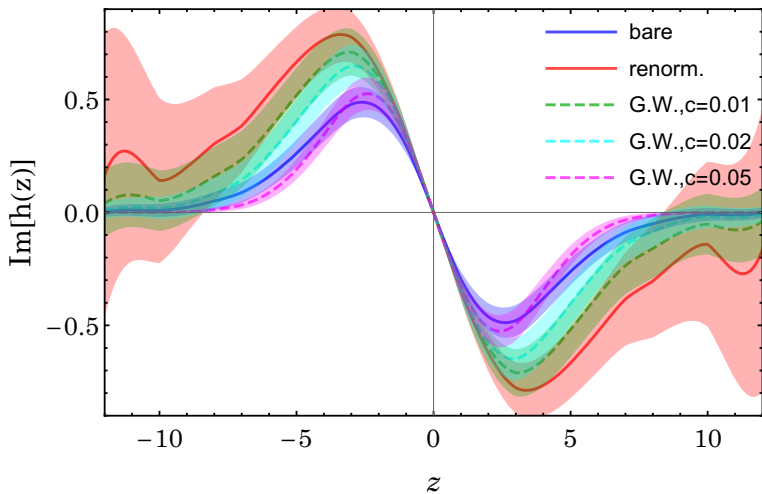
Jianhui Zhang et al. tbp

$$\begin{aligned}\tilde{q}_{GW}(x, \Lambda, p^z) &= \int \frac{dz}{4\pi} e^{ixp^z z - z^2/a^2} \langle p | \bar{\psi}(0, 0_\perp, z) \gamma^z L(z, 0) \psi(0) | p \rangle \\ &= \int_{-1}^1 \frac{du}{|u|} \int dy Z\left(\frac{y}{u}, \frac{\Lambda}{p^z}, \frac{\mu}{p^z}\right) \left[ \frac{ap^z}{2\sqrt{\pi}} e^{-\frac{a^2(x-y)^2 p_z^2}{4}} \right] q(u) \\ &+ \mathcal{O}(\Lambda_{\text{QCD}}^2/p_z^2, M^2/p_z^2, 1/ap^z)\end{aligned}$$

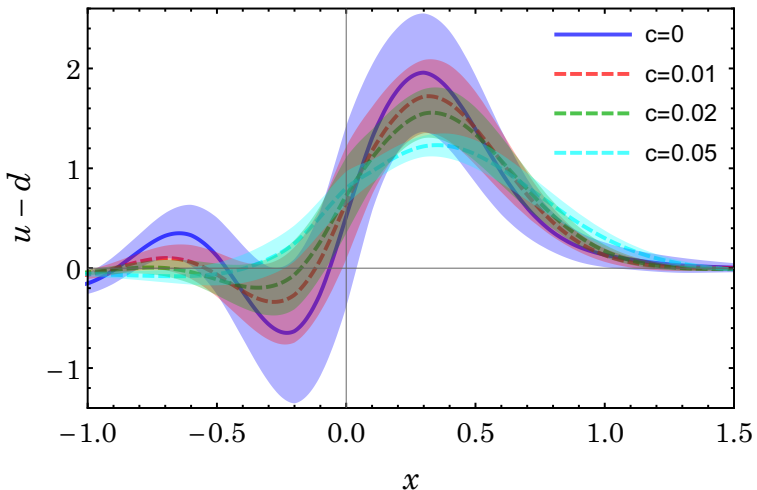
This is only an illustration. Other modifications can be more effective but will require recalculation of  $Z$ .



Real part of the correlator



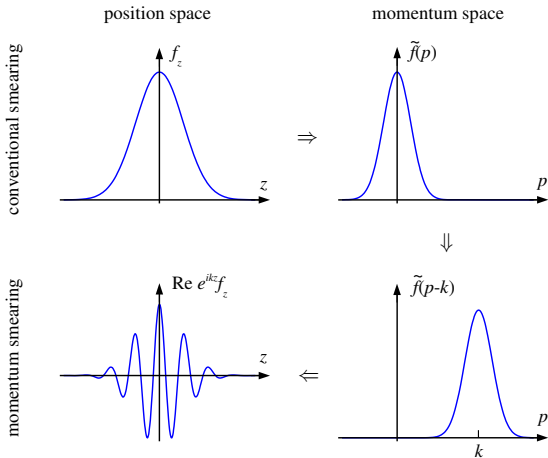
Imaginary part of the correlator



resulting quark pdf. For  $p^z \rightarrow \infty$  all have to agree

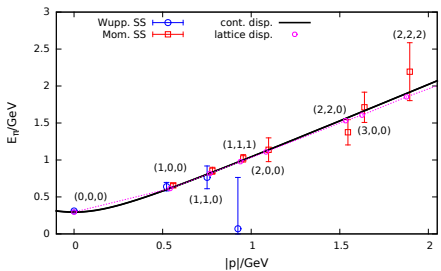
Whatever you do, reaching large momenta is the key

momentum dependent smearing: B. Musch et al., 1602.05525

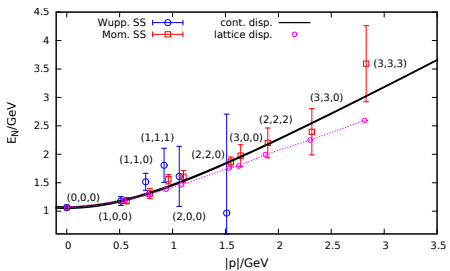


# Results

- modified smearing works great



pion



nucleon

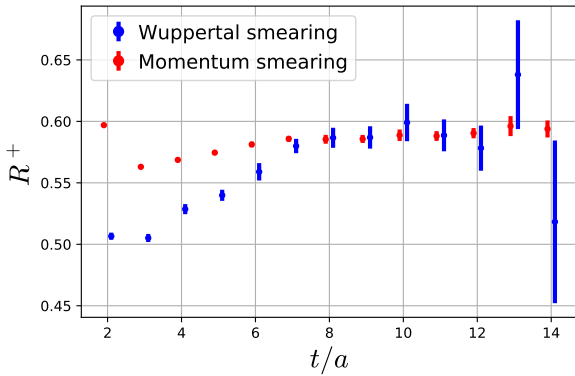
This improves also the moment method, e.g., for the pion DA  
F. Hutzler et al. 1705.10236

in the continuum

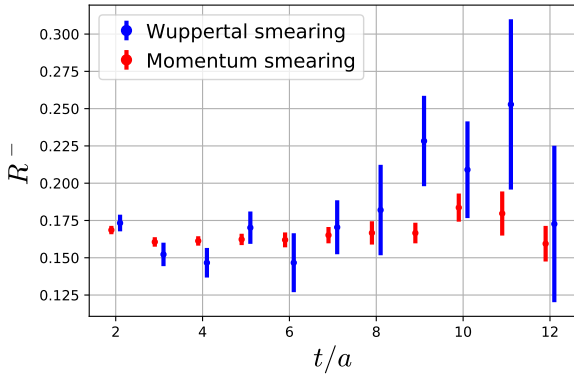
$$\begin{aligned} & \langle 0 | \bar{d}(z_2 n) \not{n} [z_2 n, z_1 n] \gamma_5 u(z_1 n) | \pi^+(p) \rangle \\ &= i f_\pi(p \cdot n) \int_0^1 dx e^{-i(z_1 x + z_2(1-x))p \cdot n} \phi(x, \mu^2), \\ \langle \xi^n \rangle &= \int_0^1 dx (2x - 1)^n \phi(x, \mu^2) \\ \phi(x, \mu^2) &= 6x(1-x) \left[ 1 + \sum_{n=1}^{\infty} a_n(\mu^2) C_n^{3/2} (2x - 1) \right] \end{aligned}$$

on the lattice:

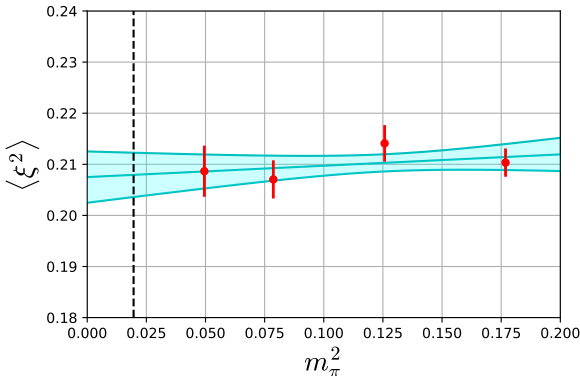
$$\begin{aligned} C_{\rho\mu\nu}^{\pm}(t, \mathbf{p}) &= a^3 \sum_{\mathbf{x}} e^{-i\mathbf{px}} \langle \mathcal{O}_{\rho\mu\nu}^{\pm}(\mathbf{x}, t) J^\dagger(0) \rangle \\ J(x) &= \bar{d}(x) \gamma_5 u(x) \\ \mathcal{O}_{\rho\mu\nu}^{+}(x) &= \bar{d}(x) \left[ \overleftarrow{D}_{\{\mu} \overleftarrow{D}_{\nu} + 2 \overleftarrow{D}_{\{\mu} \overrightarrow{D}_{\nu} + \overrightarrow{D}_{\{\mu} \overrightarrow{D}_{\nu}} \right] \gamma_{\rho\}} \gamma_5 u(x) \\ \mathcal{O}_{\rho\mu\nu}^{-}(x) &= \bar{d}(x) \left[ \overleftarrow{D}_{\{\mu} \overleftarrow{D}_{\nu} - 2 \overleftarrow{D}_{\{\mu} \overrightarrow{D}_{\nu} + \overrightarrow{D}_{\{\mu} \overrightarrow{D}_{\nu}} \right] \gamma_{\rho\}} \gamma_5 u(x), \\ \mathcal{R}_{4ij}^{\pm} &= \frac{C_{4ij}^{\pm}(t, \mathbf{p})}{C_4(t, \mathbf{p})} \\ \langle \xi^2 \rangle &= \zeta_{11} R^- + \zeta_{12} R^+ \quad \text{renormalization} \end{aligned}$$



The improved errors for  $R^+$  on H105



The improved errors for  $R^-$  on H105



The resulting on H105  
Note: No continuum extrapolation yet

(2) We have invested most effort into a formulation other than LaMET:

V. Braun nad D. Müller EPJ C55 (2008) 349; arXiv:0709.1348

advantages:

- physical current operators; no renormalization of Wilson line needed
- avoids lattices axes, large discretization errors
- control of higher twist effects
- no matching function needed
- no unclear systematic uncertainties

disadvantage:

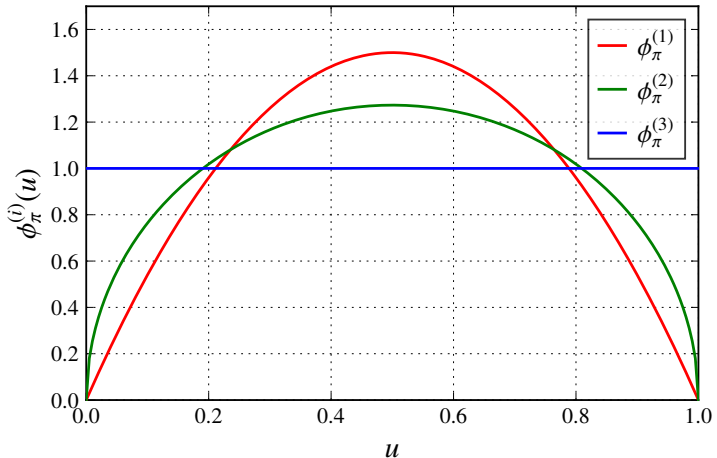
- more work is needed to obtain suggestive results. The total amount of work needed to get reliable and phenomenologically relevant results is probably the same for all variants.

Start from non-local correlators to analyse, e.g., the pion distribution amplitude

$$\begin{aligned}\langle 0 | T\{j_\mu(x)j_\nu(-x)\} |\pi^0(p) \rangle &= -\frac{5i}{p} f_\pi \epsilon_{\mu\nu\rho\sigma} \frac{x^\rho p^\sigma}{8\pi^2 x^4} T(p \cdot x, x^2) \\ T(p \cdot x, x^2) &= \int_0^1 du \quad e^{i(2u-1)p \cdot x} \quad H(u, (\mu x)^2, \alpha_s(\mu)) \Phi_\pi(u, \mu) \\ &\quad + \text{higher twist}\end{aligned}$$

$H$  short distance coefficient function, pQCD

It is completely sufficient to study  $x^0 = 0$ ,  $\vec{x} \neq 0$  **IF**  $|\vec{x}|$  is small enough for pQCD to apply.

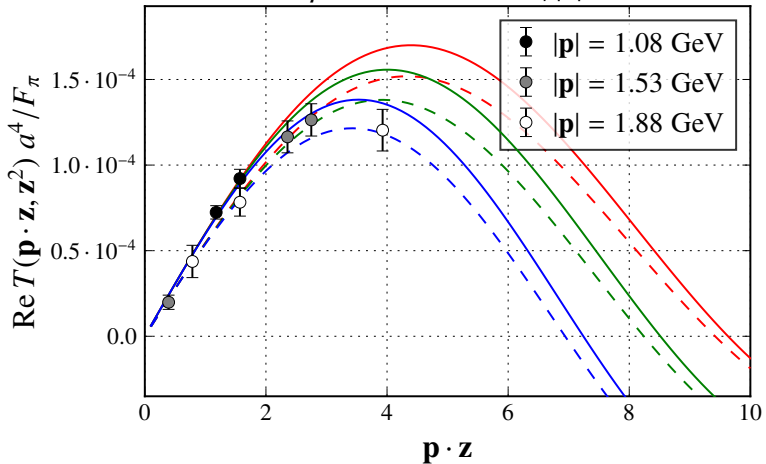


### Three model DAs for the pion

$$\phi_{\pi}^{(1)}(u) = 6u(1-u), \quad \phi_{\pi}^{(2)}(u) = \frac{8}{\pi} \sqrt{u(1-u)}, \quad \phi_{\pi}^{(3)}(u) = 1$$

The real part of  $T \leftarrow$  pion distribution amplitude:

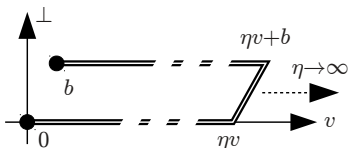
$$\mu = 0.95 \text{ GeV} = 2/|\mathbf{z}|$$



solid/dashed: with/without HT corrections; not yet continuum extrapolated

TMDs are related to correlators of the type

$$\tilde{\Phi}_{\text{unsubtr.}}^{[\Gamma]}(b, P, S, \dots) \equiv \frac{1}{2} \langle P, S | \bar{q}(0) \Gamma \mathcal{U}[0, \eta v, \eta v+b, b] q(b) | P, S \rangle$$



We simulate for spatial, not light-like separations, but the limit  $\hat{\zeta} \rightarrow \infty$  of

$$\hat{\zeta} := \frac{v \cdot P}{\sqrt{v^2} \sqrt{P^2}}$$

reproduces the light-cone behavior.

We used RBC/UKQCD (domain wall) and W&M (Clover) ensembles,  $N_f = 2 + 1$

ID	Clover	DWF
Fermion Type	Clover	Domain-wall
Geometry	$32^3 \times 96$	$32^3 \times 64$
$a(\text{fm})$	0.11403(77)	0.0840(14)
$m_\pi(\text{MeV})$	317(2)(2)	297(5)
# confs.	967	533
# meas.	23208	4264

only connected diagrams, i.e.  $u - d$

$$\begin{aligned}
\tilde{\Phi}_{\text{subtr.}}^{[\Gamma]}(b, P, S, \dots) &= \tilde{\Phi}_{\text{unsubtr.}}^{[\Gamma]}(b, P, S, \dots) \cdot \mathcal{S} \cdot Z_{\text{TMD}} \cdot Z_2 \\
\Phi^{[\Gamma]}(x, \mathbf{k}_T, P, S, \dots) &= \int \frac{d^2 \mathbf{b}_T}{(2\pi)^2} \int \frac{d(b \cdot P)}{2\pi P^+} e^{ix(b \cdot P) - i\mathbf{b}_T \cdot \mathbf{k}_T} \tilde{\Phi}_{\text{subtr.}}^{[\Gamma]} \Big|_{b^+=0} \\
\Phi^{[\gamma^+]} &= f_1 - \frac{\epsilon_{ij} \mathbf{k}_i \mathbf{S}_j}{m_N} f_{1T}^\perp \\
\Phi^{[\gamma^+ \gamma^5]} &= \Lambda g_1 + \frac{\mathbf{k}_T \cdot \mathbf{S}_T}{m_N} g_{1T} \\
\Phi^{[i\sigma^{i+} \gamma^5]} &= \mathbf{S}_i h_1 + \frac{(2\mathbf{k}_i \mathbf{k}_j - \mathbf{k}_T^2 \delta_{ij}) \mathbf{S}_j}{2m_N^2} h_{1T}^\perp + \frac{\Lambda \mathbf{k}_i}{m_N} h_{1L}^\perp + \frac{\epsilon_{ij} \mathbf{k}_j}{m_N} h_1^\perp \\
\tilde{f}^{[m](n)}(\mathbf{b}_T^2, \dots) &= n! \left( -\frac{2}{m_N^2} \partial_{\mathbf{b}_T^2} \right)^n \int_{-1}^1 dx x^{m-1} \int d^2 \mathbf{k}_T e^{i\mathbf{b}_T \cdot \mathbf{k}_T} f(x, \mathbf{k}_T^2) \\
\langle \vec{k}_y \rangle_{TU}(\mathbf{b}_T^2; \dots) &= m_N \frac{\tilde{f}_{1T}^{\perp [1](1)}(\mathbf{b}_T^2; \dots)}{\tilde{f}_1^{[1](0)}(\mathbf{b}_T^2; \dots)}
\end{aligned}$$

## the generalized tensor charge

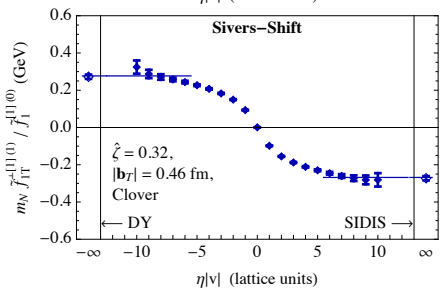
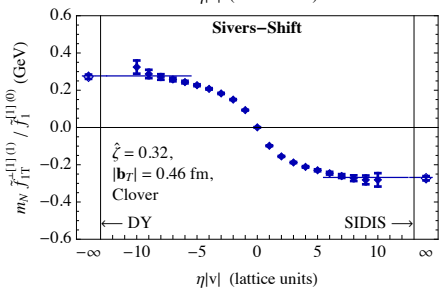
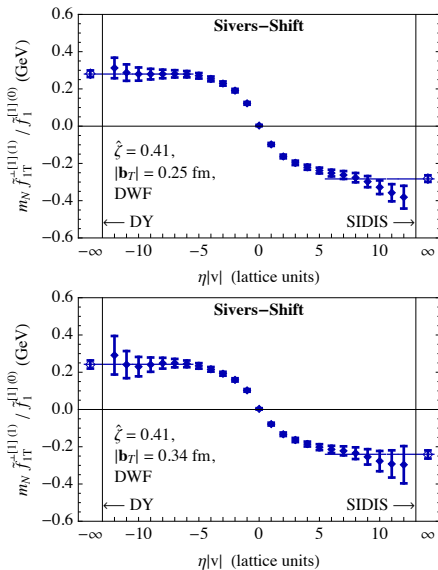
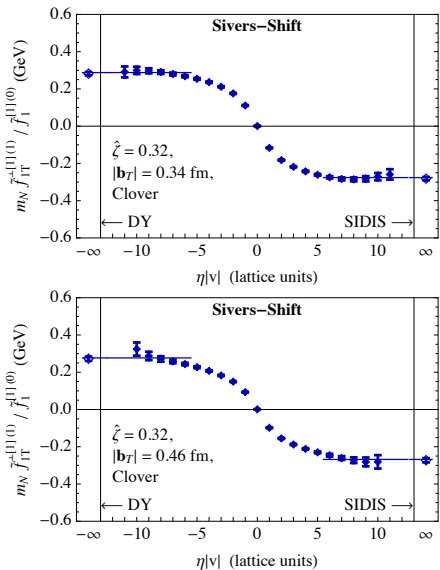
$$\tilde{h}_1^{[1](0)}(\mathbf{b}_{\mathrm{T}}^2; \dots) / \tilde{f}_1^{[1](0)}(\mathbf{b}_{\mathrm{T}}^2; \dots)$$
$$g_T^{u-d} = \int dx d^2\mathbf{k}_{\mathrm{T}} h_1(x, \mathbf{k}_{\mathrm{T}}^2) = \tilde{h}_1^{[1](0)}(\mathbf{b}_{\mathrm{T}}^2 = 0)$$

limits:

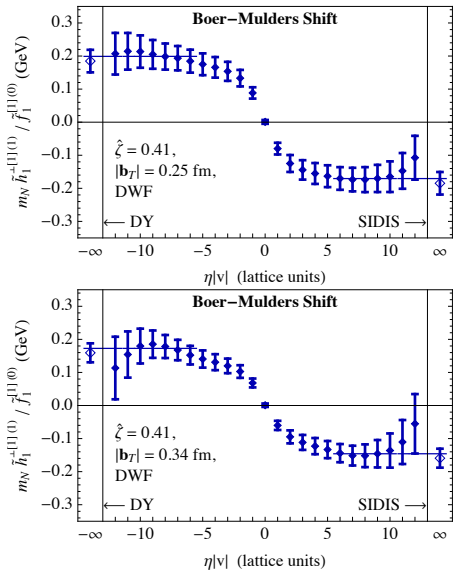
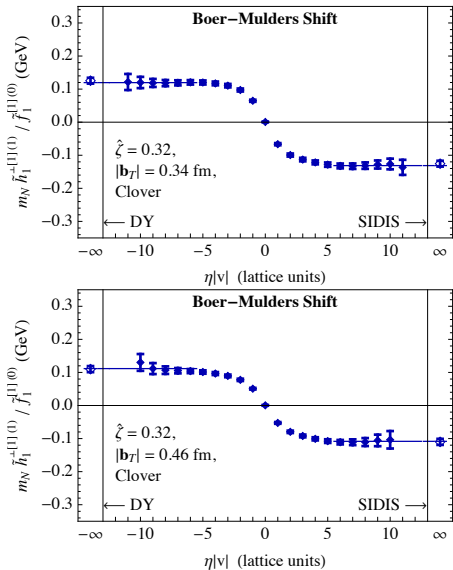
$$\eta|v| \rightarrow \infty$$

$$b_T \gg a$$

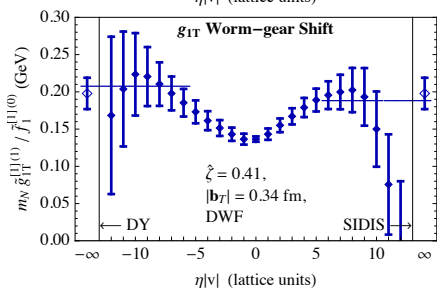
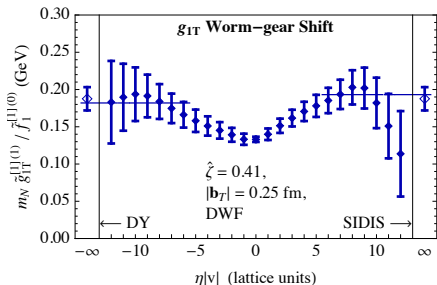
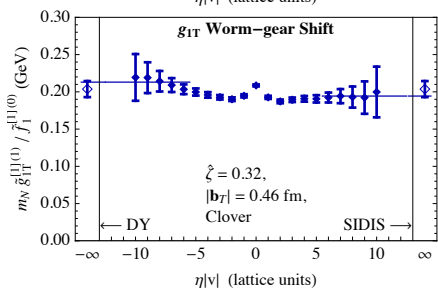
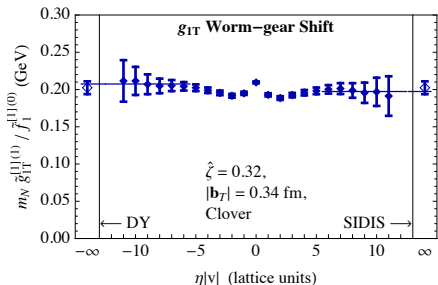
$$\hat{\zeta} \rightarrow \infty$$



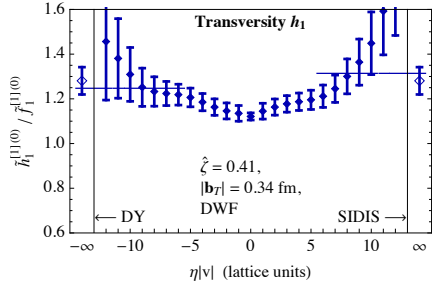
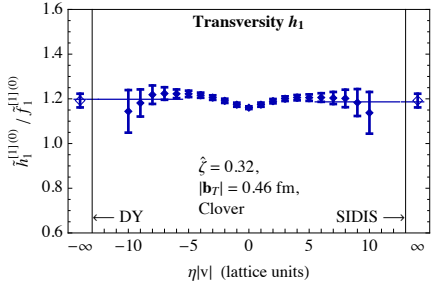
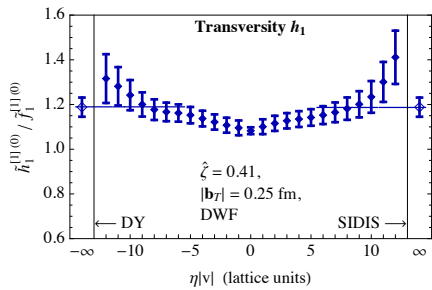
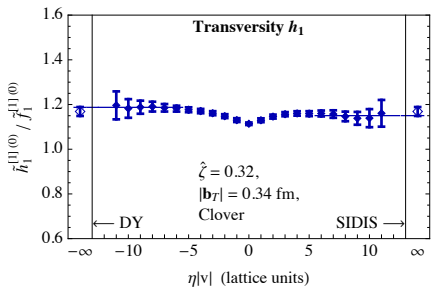
## Sivers shift



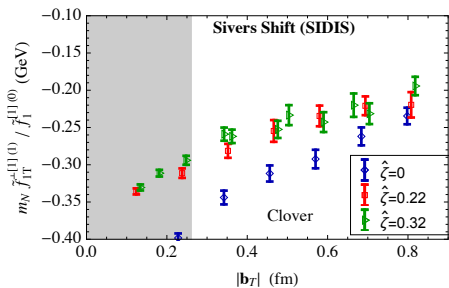
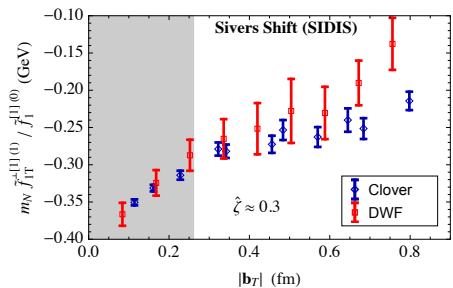
## Boer–Mulders shift



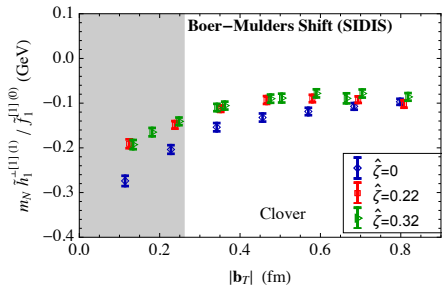
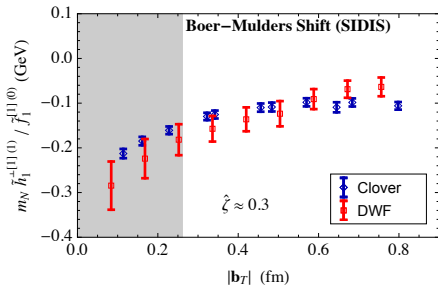
Worm-gear shift, for  $g_{1T}$



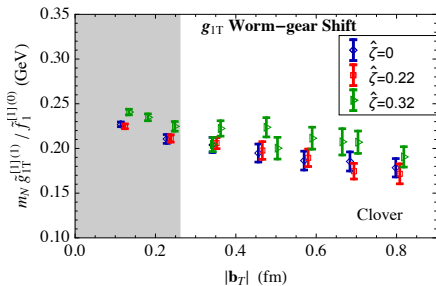
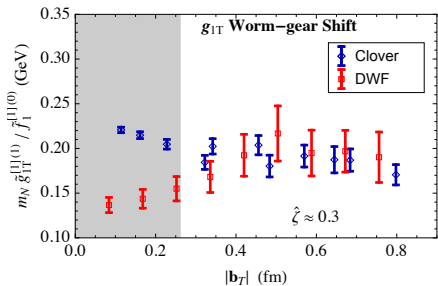
transversity ratio



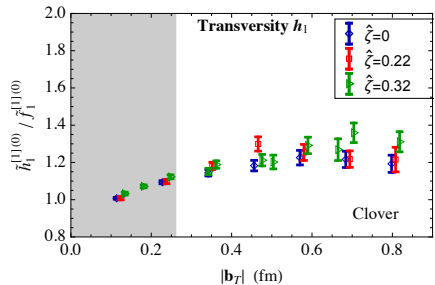
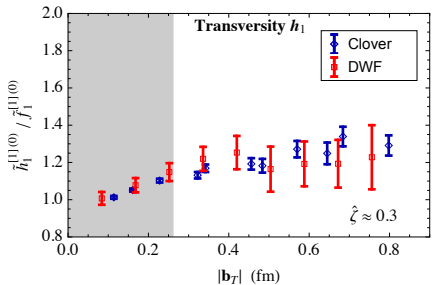
## Sivers shift



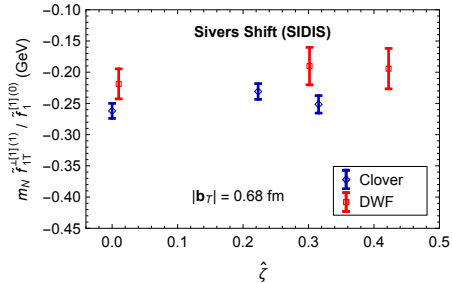
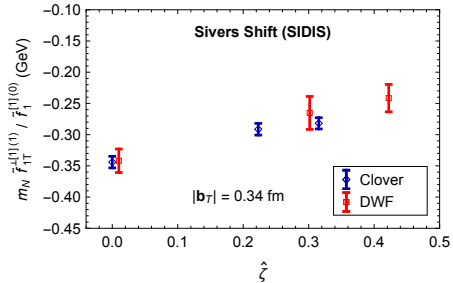
## Boer–Mulders shift



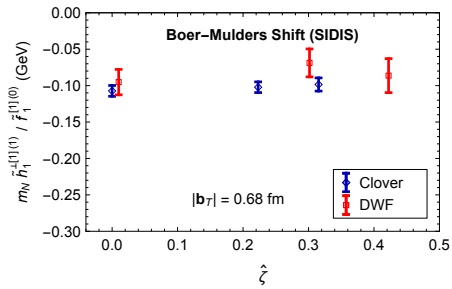
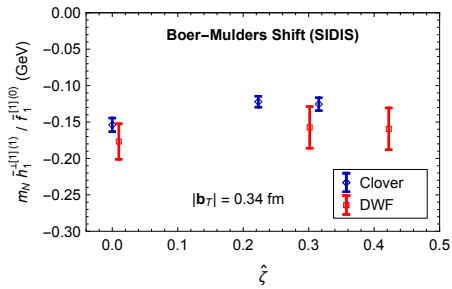
Worm-gear shift, for  $g_{1T}$



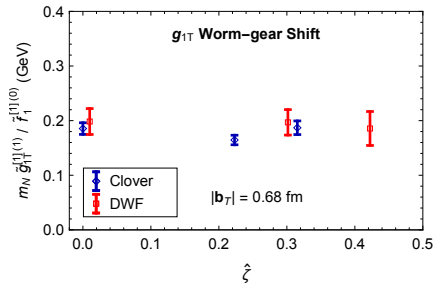
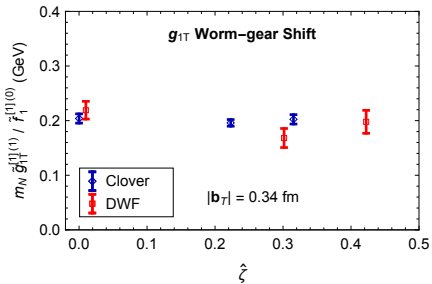
transversity ratio



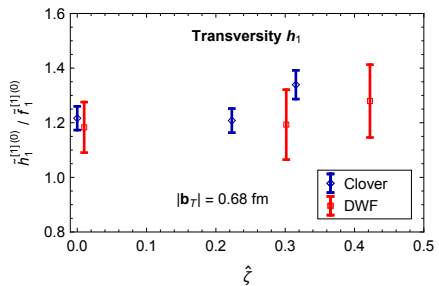
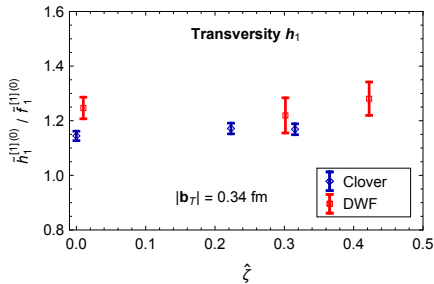
Sivers shift



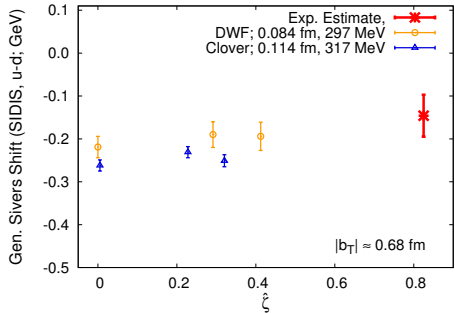
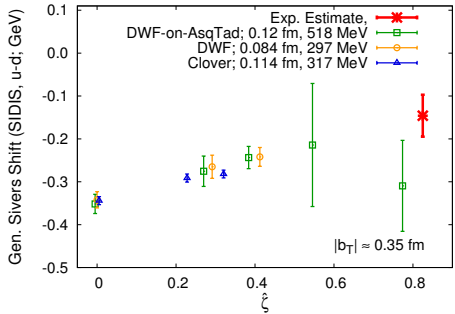
## Boer-Mulders shift



Worm-gear shift, for  $g_{1T}$



transversity ratio

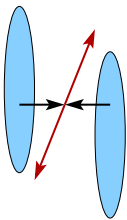


Comparison with experiment

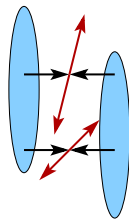
# Double Parton Distributions and MPIs at LHC

M- Diehl et al.

Full use of discovery potential requires a better of the “underlying event”, example: Double hard interactions



Single parton interaction



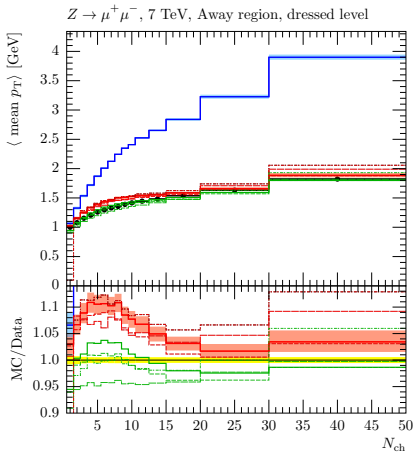
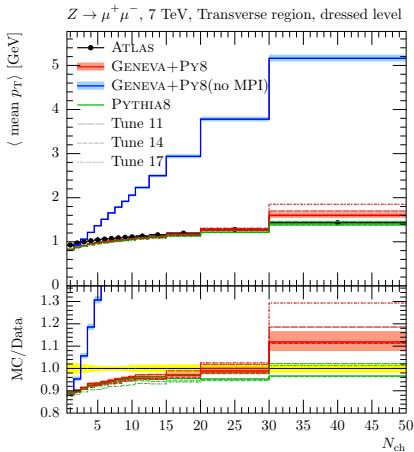
Double parton interaction

Naive (?) assumption

$$d\sigma_{DPS} = \frac{d\sigma_{SPS} d\sigma_{SPS}}{2\sigma_{eff}}$$

Two plots from Alioli, Bauer, Guns, Tackmann 1605.07192  
mean charged particle  $p_T$  as function of  $N_{ch}$ .

Events with large  $N_{ch}$  have a higher MPI contribution. MPIs produce many particles with  $p_T$  of  $O(1 \text{ GeV})$ .



Quark-quark correlations in the pion; RQCD;  $N_f = 2$ ,  
 Clover-Wilson fermions, down to nearly physical mass  
 $(m_\pi = 150 \text{ MeV})$ .

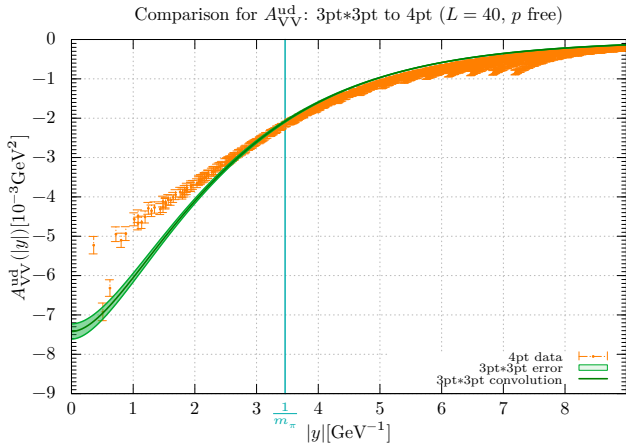
Many direct Tests of naive factorization, e.g., Integrals based on

$$\int 4pt - \text{correlator} \stackrel{?}{=} \int (\text{formfactor})^2$$

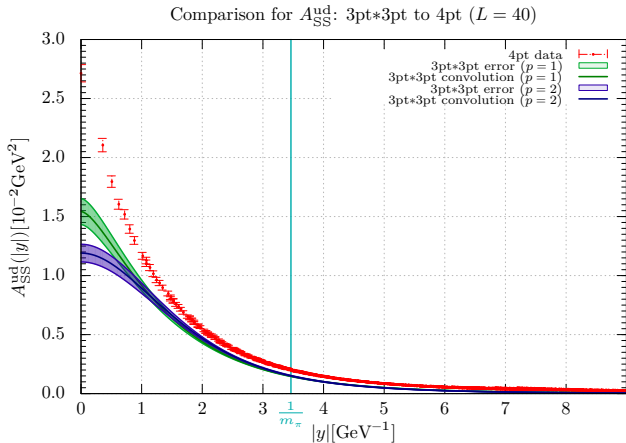
$$\begin{aligned} \int_{-\infty}^{\infty} d(\vec{p}_\perp \cdot \vec{y}_\perp) A_{VV}(y^2, py) &= \frac{1}{2p^+} \int_{-\infty}^{\infty} dy^- \langle \pi(p) | V^+(0) V^+(y) | \pi(p) \rangle \Big|_{y^+=0} \\ \int_{-\infty}^{\infty} d(py) A_{VV}^{ud}(y^2, yp) &\approx - \int \frac{d^2 r_\perp}{(2\pi)^2} e^{-i\vec{y}_\perp \cdot \vec{r}_\perp} |F_V(r^2)|^2 \end{aligned}$$

Quark-quark correlations in the pion are sizeable. On theoretical grounds they should be stronger in nucleons.

## Direct tests of naive factorization: Test 1 VV case



## Direct tests of naive factorization: Test 1 SS case

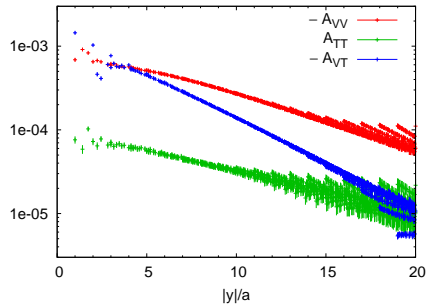
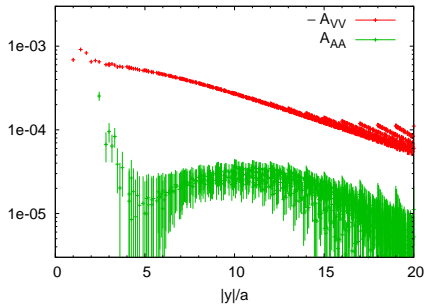


## Spin correlations

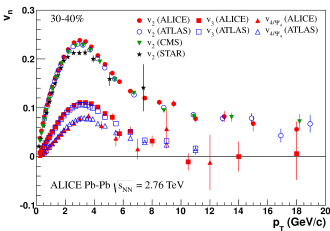
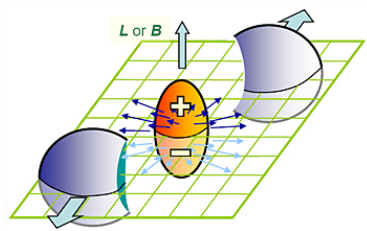
AA: longitudinal spin correlation  $u^\uparrow \bar{d}^\uparrow + u^\downarrow \bar{d}^\downarrow - u^\uparrow \bar{d}^\downarrow - u^\downarrow \bar{d}^\uparrow$

TT: transverse spin correlation  $\vec{s}_u \cdot \vec{s}_d$

VT:  $\vec{y} \cdot \vec{s}_{\bar{d}}$



## Key question of relativistic heavy ion physics:

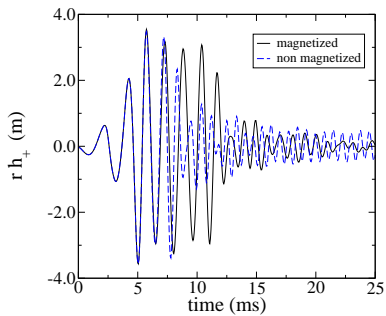
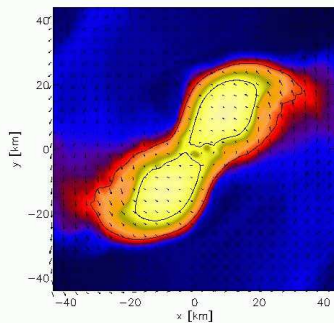


In HICs one produces the strongest magnetic fields in the universe

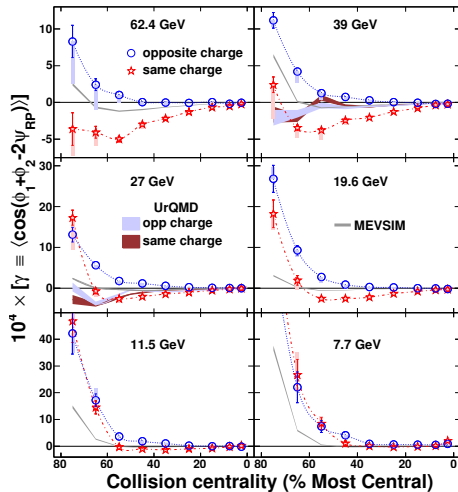
- Does this influence thermalization ?
- Does this lead to novel effects like the CME ?

## relevance of QCD & magnetic fields for astrophysics

arXiv:0801.4387 gravitational wave signal from neutron star merger



Lee, Fukushima, Kharzeev et al.: The QCD chiral anomaly  $G^{\mu\nu}\tilde{G}_{\mu\nu} \sim \vec{E}_{\text{color}} \cdot \vec{B}_{\text{color}}$  can induce an electromagnetic  $\vec{E}$  parallel or antiparallel to  $\vec{B}$ . STAR 1404.1433 :



## Magnetic field on the Lattice

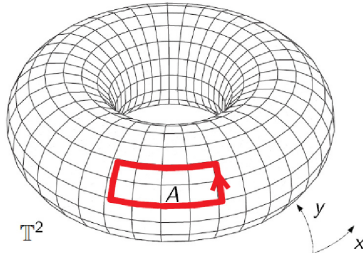
QCD is contained in the generating functional:

$$Z[J_\mu^a, \bar{\eta}^i, \eta^i] = \int \mathcal{D}[A^{a\mu}, \bar{\psi}^i, \psi^i] \exp \left( i \int d^4x \left[ \mathcal{L}_{\text{QCD}} - J_\mu^a A_\mu^a - \bar{\psi}^i \eta^i - \bar{\eta}^i \psi^i \right] \right)$$

Discretized space time  $\Rightarrow$  e.g. the Wilson action

$$\begin{aligned} U(l_1) &= \exp \left( -ig A^b(l_1) \frac{\lambda^b}{2} a \right) \\ W_{\square} &= \text{Tr}\{U(l_1)U(l_2)U(l_3)U(l_4)\} \\ \sum_{\square} \frac{2}{g^2} (3 - \mathcal{R}e W_{\square}) &= \frac{1}{4} \int d^4x \left( F_{\mu\nu}^a F_{\mu\nu}^a + O(a^2) \right) \end{aligned}$$

## Magnetic field on the torus with surface area $L_x L_y$



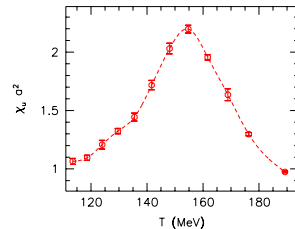
- phase factor for a charged particle transported along path  
 $\mathcal{C}$ :  $\exp(iq \oint_C x_\mu A_\mu)$
- Stokes theorem:  $\int_C dx_\mu A_\mu = \int \int_A d\sigma B = B \cdot A$   
but also  
 $= - \int \int_{T^2 - A} d\sigma B = -B \cdot (L_x L_y - A)$
- equality of phase factors gives quantization condition  
[Hashimi, Wiese '09]

$$\exp(iqBL_x L_y) = 1 \quad \rightarrow \quad qBL_x L_y = 2\pi \cdot N_b, \quad N_b \in \mathbb{Z}$$

## Transition characteristics

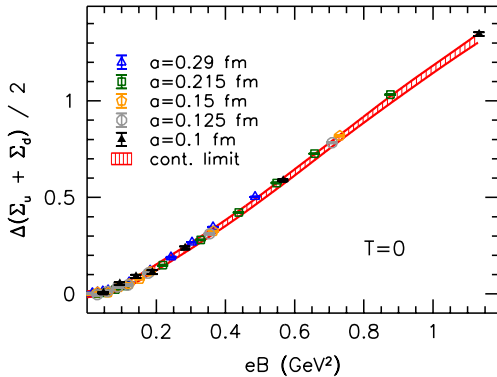
- chiral susceptibility  
( $\sim$  specific heat)

$$\chi = \frac{\partial^2 \log Z}{\partial m^2} \quad (1)$$

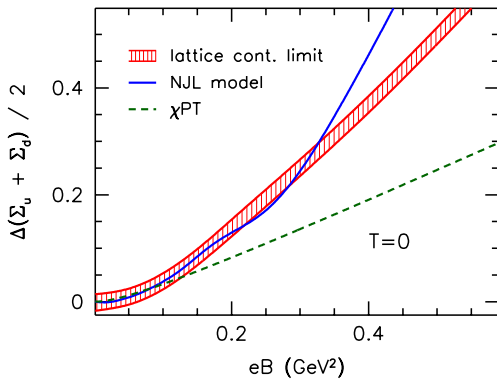


- transition temperature: peak maximum
- order of transition: volume-dependence of height  
 $h(V) \propto V^\alpha$   
1st ( $\alpha = 1$ ), 2nd ( $0 < \alpha < 1$ ) or crossover ( $\alpha = 0$ )

- magnetic catalysis at zero temperature is a robust concept:  
 $\chi$ PT, NJL model, AdS-CFT, linear  $\sigma$  model, ...

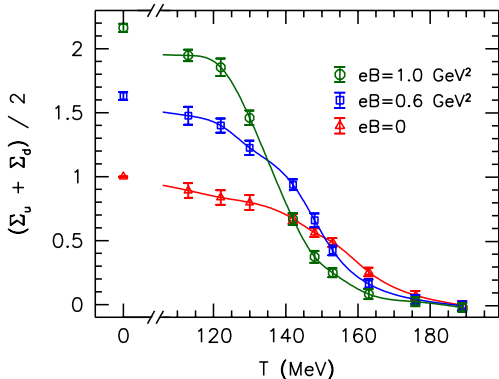


- magnetic catalysis at zero temperature is a robust concept:  
 $\chi$ PT, NJL model, AdS-CFT, linear  $\sigma$  model, ...



## Inverse magnetic catalysis

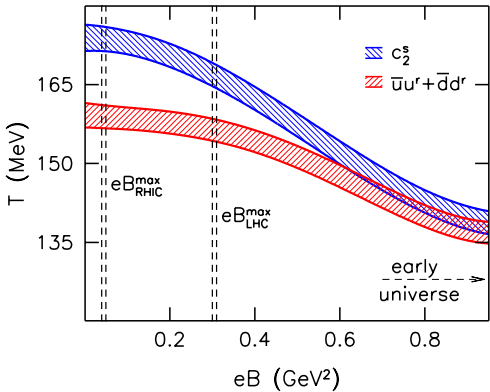
- lattice QCD, physical  $m_\pi$ , continuum limit [Bali et al '11, '12]



- at  $T \approx 150$  MeV the condensate is reduced by  $B$   
dubbed ‘inverse magnetic catalysis’

## Phase diagram

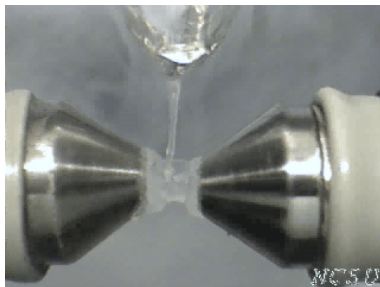
- inflection point of  $\bar{\psi}\psi(T)$  defines  $T_c$
- significant difference whether IMC is exhibited or not:



lattice QCD, physical  $m_\pi$ , continuum limit [Bali et al '11]

## Matter in magnetic fields (linear response)

- paramagnets: attracted by magnetic field
- diamagnets: repel magnetic field

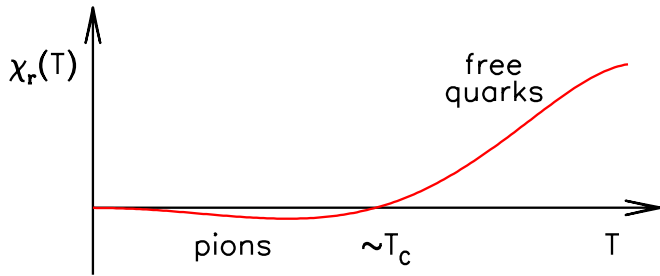


paramagnet: liquid oxygen

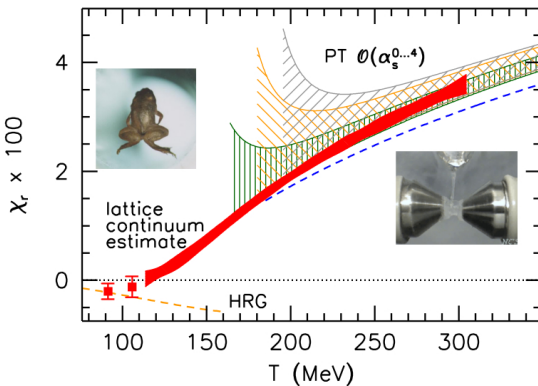
diamagnet: frog

- is thermal QCD as a medium para- or diamagnetic?

fermions give paramagnetic behaviour, bosons diamagnetic  
⇒ Expectation for the susceptibility



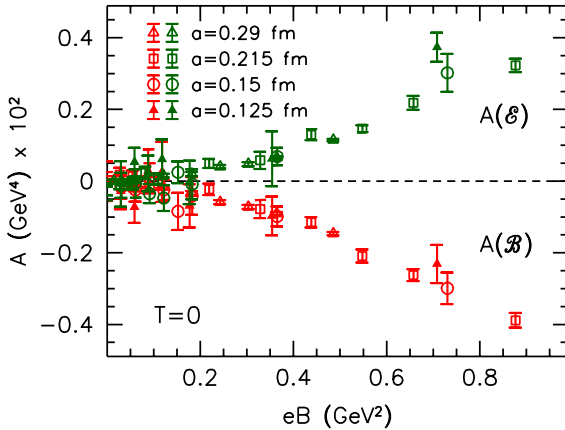
## Susceptibility from the lattice



- comparison to Hadron Resonance Gas model (low  $T$ ) and to perturbation theory (high  $T$ )
- The quark gluon plasma is paramagnetic

## Other results: Gluon anisotropies 1303.1328

$$A(\mathcal{E}) = \frac{T}{V} \left\langle \frac{\beta}{6} \sum_n \left( \text{tr } \mathcal{E}_\perp^2(n) - \text{tr } \mathcal{E}_\parallel^2(n) \right) \right\rangle$$



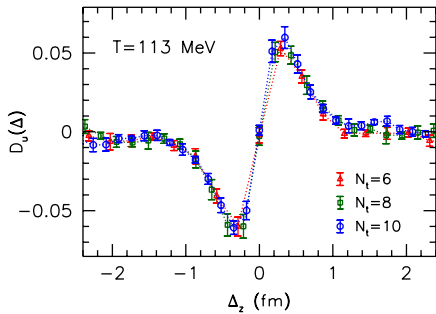
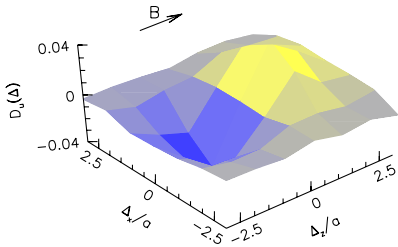
# The correlation between topological charge and electric current

1401.4141

$$J_\nu^f(x) = \bar{\psi}_f \gamma_\nu \psi_f(x)$$

$$D_f(\Delta) = \frac{\langle q_{\text{top}}(x) \cdot J_t^f(x + \Delta) \rangle}{\sqrt{\langle q_{\text{top}}^2(x) \rangle} \langle \Sigma_{xy}^f(x) \rangle}}$$

**lattice results:**



# Conclusions

- RQCD investigates a very broad spectrum of problems with large computer resources
- PDFs, GPDs, DPDs, TMDs, ...
- The frontier is the continuum limit  $\Rightarrow$  CLE open boundary conditions
- No solution yet for  $\langle x(u - d) \rangle$
- encouraging results for alternative lattice approaches
- QCD in a magnetic field is a fascinating topic